Journal of Structural Geology 32 (2010) 1271–1278

Contents lists available at ScienceDirect

Journal of Structural Geology

journal homepage: www.elsevier.com/locate/jsg

Quantifying uncertainties in multi-scale studies of fractured reservoir analogues: Implemented statistical analysis of scan line data from carbonate rocks

Vincenzo Guerriero [a,*], Alessandro Iannace [a], Stefano Mazzoli [a], Mariano Parente [a], Stefano Vitale [a], Maurizio Giorgioni [b]

[a] Dipartimento di Scienze della Terra, Università degli studi di Napoli 'Federico II', Largo San Marcellino 10, 80138 Napoli, Italy
[b] Shell Italia E & P, Rome, Italy

ARTICLE INFO

Article history:
Received 13 March 2008
Received in revised form
10 April 2009
Accepted 27 April 2009
Available online 8 May 2009

Keywords:
Structural analysis
Fracture statistics
Power-law distribution
Confidence interval

ABSTRACT

In this study we performed a fracture analysis on a Cretaceous bedded carbonate succession well exposed in the Sorrento Peninsula. The studied succession includes stratigraphic units that are very similar to the productive units of the buried Apulian Platform reservoir rocks in southern Italy. We analyzed eight carbonate beds, including both limestones and dolomites. The basic technique used in this study consisted of measuring fractures along bedding-parallel scan lines. For one limestone bed, a microscale scan line, about 15 cm long, was also analyzed using a digital microcamera. Provided the cumulative distribution of fracture apertures is well described by a power law, our analysis shows how the uncertainty in the estimate of fracture aperture cumulative frequencies grows for large aperture values. This feature results in a large uncertainty in the estimate of the slope of the least-squares line (in a bi-logarithmic diagram) approximating the data distribution, which is the exponent of the power law. As the latter represents a fundamental parameter characterizing a fracture set and fracture distribution over different scales, reducing the uncertainty in the estimate of the slope of the curve represents an important objective of quantitative fracture analysis. This is obtained in this study by the application of multi-scale analysis, and by integrating micro-scan line data with classic outcrop-based scan line analysis. The quantification of uncertainties in the cumulative distribution estimates of fracture apertures is performed by analyzing in detail the spacing distribution – and consequently fracture-density distribution – for each aperture value. Our results suggests that a meaningful statistical analysis of fracture attributes such as aperture (or opening displacement) may be effectively carried out by using properly determined confidence intervals and by the integration of outcrop-based and micro-scan line data sets.

1. Introduction

A fundamental issue in the characterization of fractured reservoirs is constituted by the limitations inherited in fracture sampling in the subsurface, as represented in well log data or cores. Fracture scaling relationships may be effectively used to overcome such limitations. Numerous studies have shown that, besides the largely studied scaling behaviour of faults, also opening-mode (i.e. Mode I) fracture size distributions are generally effectively described by a power law – i.e. parameters such as length or opening of fractures are self-similar over a range of scales (e.g. Das Gupta, 1978; Sinclair, 1980; Mandelbrot, 1983; Nelson, 1985; Gudmundsson, 1987; Heffer and Bevan, 1990; Barton and Zoback, 1992; Gillespie et al., 1993; Sanderson et al., 1994; Barton, 1995; Gross and Engelder, 1995; Johnston and McCaffrey, 1996; Marrett, 1997; Odling et al., 1999; Ortega and Marrett, 2000, 2006). On the other hand, fracture spacing appears to be controlled by a series of parameters including (Nelson, 1985): (i) rock composition; (ii) rock texture, grain size, porosity; (iii) structural position; and (iv) mechanical layer thickness. The latter parameter has been extensively analyzed, and the relationship of increasing fracture spacing for increasing bed thickness has been widely documented (Price, 1966; Huang and Angelier, 1989; Narr and Suppe, 1991; Gross, 1993; Mandal et al., 1994; Gross and Engelder, 1995; Wu and Pollard, 1995; Narr, 1996; Pascal et al., 1997; Bai and Pollard, 2000). Although most of the studies on fracture populations concerned fracture spacing or fracture length, fracture-opening distributions have also been effectively analyzed, confirming that the cumulative distribution of joint apertures is well described by a power law (Ortega et al., 1998, 2006; Ortega and Marrett, 2000). In order to further clarify the meaning and importance of power-law distributions, an example

* Corresponding author.
E-mail address: vincenzo.guerriero@unina.it (V. Guerriero).

0191-8141/$ – see front matter © 2009 Elsevier Ltd. All rights reserved.
doi:10.1016/j.jsg.2009.04.016

may be used, emphasizing some of the main quantities that can be obtained. Suppose that the cumulative distribution of joint apertures for a fracture set is described by the following power law:

$$F(b) = c \cdot b^{-m}, \quad (1)$$

where b is the joint aperture, F is the cumulative frequency (i.e. the number of joints per meter having aperture greater than b), c and m are experimental constants.

Let us consider the mean aperture b^* between two arbitrary limits b_1 and b_2:

$$b^* = \int_{b1}^{b2} b \cdot f(b)\, db \quad (2)$$

where $f(b)$ is the aperture frequency distribution, given by the derivative of $F(b)$. This non-dimensional quantity provides the contribution, given by those joints for which $b_1 < b < b_2$, to the longitudinal strain of the rock. Furthermore equation (2), providing the 'void' fraction estimate along the scan line for any values of b_1 and b_2, could furnish significant information about the porosity and permeability of the rock at different scales of observation. It should also be noted that the value $m = 1$, represents a 'critical value', because it is well known from mathematical theory that for $|m| > 1$, $b_2 = 1$ and $b_1 \to 0$, equation (2) yields: $b^* \to \infty$ (in reality, a lower limit for the validity of power the law exists, and the condition $b_1 \to 0$ has only a theoretical meaning). On the other hand, for $|m| < 1$, $b_2 \to \infty$ and $b_1 = 1$, it results: $b^* \to \infty$. The geological meaning is that $|m| > 1$ characterizes more 'pervasive' fracture sets. For $|m| > 1$, the larger contribution to fracture porosity (in case of non-filled joints), as well as longitudinal strain, is provided by the smaller fractures. Consequently fracture porosity grows slowly as the scale of observation increases. Conversely, for $|m| < 1$, fracture porosity and longitudinal strain increase markedly with the scale of observation.

In outcrop-based studies, the parameters (e.g. fracture spacing/fracture length, fracture aperture) for fracture analysis are generally acquired by a widely used methodology involving the statistical analysis of fracture sets detected along scan lines. Despite the large amount of work carried out using this methodology, very few studies deal with the reliability of scan line data interpretation, especially concerning the quantification of uncertainties. In order to normalize data acquisition by this methodology, hence allowing for comparison between data gathered at different locations, Ortega et al. (2006) proposed the use of a common fracture size threshold, requiring the determination of fracture size distribution. The latter Authors proposed the analysis of the standard deviation of consecutive fracture frequency estimates as a means to evaluate the uncertainty of fracture-density determinations.

The aim of the paper is to afford the problem of fracture estimate uncertainty by analyzing the power-law distribution of fracture attributes, such as fracture opening and fracture spacing. In order to have a reliable statistical distribution, we needed to integrate naked-eye data collection with micro-observation by means of a digital microcamera directly on the field. The study has been performed on Cretaceous bedded carbonate succession cropping out in southern Italy.

2. Geological setting and fracture data collection

Significant oil discoveries in the southern Apennines fold and thrust belt are associated with hydrocarbon traps consisting of reverse-fault-related, open, long-wavelength folds involving a 6–8 km thick Mesozoic–Tertiary carbonate platform succession (Shiner et al., 2004). These carbonate platform reservoir rocks, deformed by thick-skinned reverse faults and inversion structures involving the underlying basement (Mazzoli et al., 2001, 2008), represent a tectonically buried portion of the Apulian Platform carbonates, continuous with those exposed in the Apulian promontory to the NE (Fig. 1a). The outcropping thrust belt forms a displaced allochthon that has been carried onto such a footwall of Apulian Platform foreland strata (Fig. 1c). The allochthonous units include carbonate platform and pelagic basin successions, locally covered by Neogene foredeep and/or thrust-top basin sediments. The structure at shallow levels is dominated by low-angle tectonic contacts separating the platform/slope carbonates of the Apennine Platform, in the hanging wall, from underlying pelagic basin successions (Lagonegro Units; Mazzoli et al., 2008). The carbonate succession of the Apennine Platform includes stratigraphic units that are very similar to the productive units of the buried Apulian Platform reservoir rocks in terms of age, lithology, facies, overall thickness, mechanical layer thickness of single beds, and rock texture. As such, outcrops of Apennine Platform carbonates are used for fracture analysis of reservoir analogues. This is capable of providing important information, although the different tectonic evolution and burial conditions experienced by the Apennine Platform with respect to the Apulian Platform carbonates (Mazzoli et al., 2008) need to be taken into account in a cautious application of the results in reservoir management.

The studied carbonate strata belong to the Triassic–Cenozoic shallow water carbonate succession of the Apennine Platform beautifully exposed in the Sorrento Peninsula at Monte Faito (Fig. 1a, b). We analyzed eight limestone/dolomite beds, of Lower Cretaceous (Albian) age. These are well exposed along a road cut at *Croce dell'Eremita*, on the NW slope of Monte Faito (Fig. 1b), approximately 30 km SE of Naples. These beds are part of a 50-m thick succession which has been studied in detail in terms of sedimentology, petrography, geochemistry and petrophysiscs (Galluccio et al., 2008). The succession has been selected for many analogies with productive horizons in the buried Apulia carbonates. It consists of an alternance of tight limestones and early diagenetic dolomites characterized by several exposure surfaces witnessed by clay levels and silicified evaporites as well as by a sharp transition to slope conglomerates (Fig. 1b).

The analyzed beds are all within a limited range of thickness (Table 1). In fact, these beds have been selected in order to minimize the effect of the most fundamental parameter – i.e. mechanical layer thickness – controlling fracture density. The limestone beds (1, 57, 107) are characterized by a mud-rich texture (wackestone and mud-dominated packstone) and show very low mean porosity (He-porosity 1.91%). The dolomite beds (66, 71, 102, 118, 120) comprise both meso- and macro-crystalline textures, with slightly higher mean porosity (He-porosity 3.01%).

The basic structure detection technique used in this study consisted of measuring fractures along bedding-parallel linear traverses (scan lines; Fig. 2). The following characteristics have been recorded for each detected fracture: type of feature (vein or joint), distance from scan line origin, attitude, length, opening displacement, morphology, crosscutting relationships, composition and texture of fracture fill, and mechanical layer thickness. The analyzed beds are characterized by one, or sometimes two, well-developed fracture sets (Fig. 3). Where two fracture sets are present, these are generally at a high angle to each other (note that there is generally a good three-dimensional exposure, permitting inspection of top and/or bottom bedding surfaces while measuring along each bedding-parallel scan line). Opening displacement (or kinematic aperture; hereafter simply termed aperture) has been recorded using the logarithmically graduated comparator of Ortega

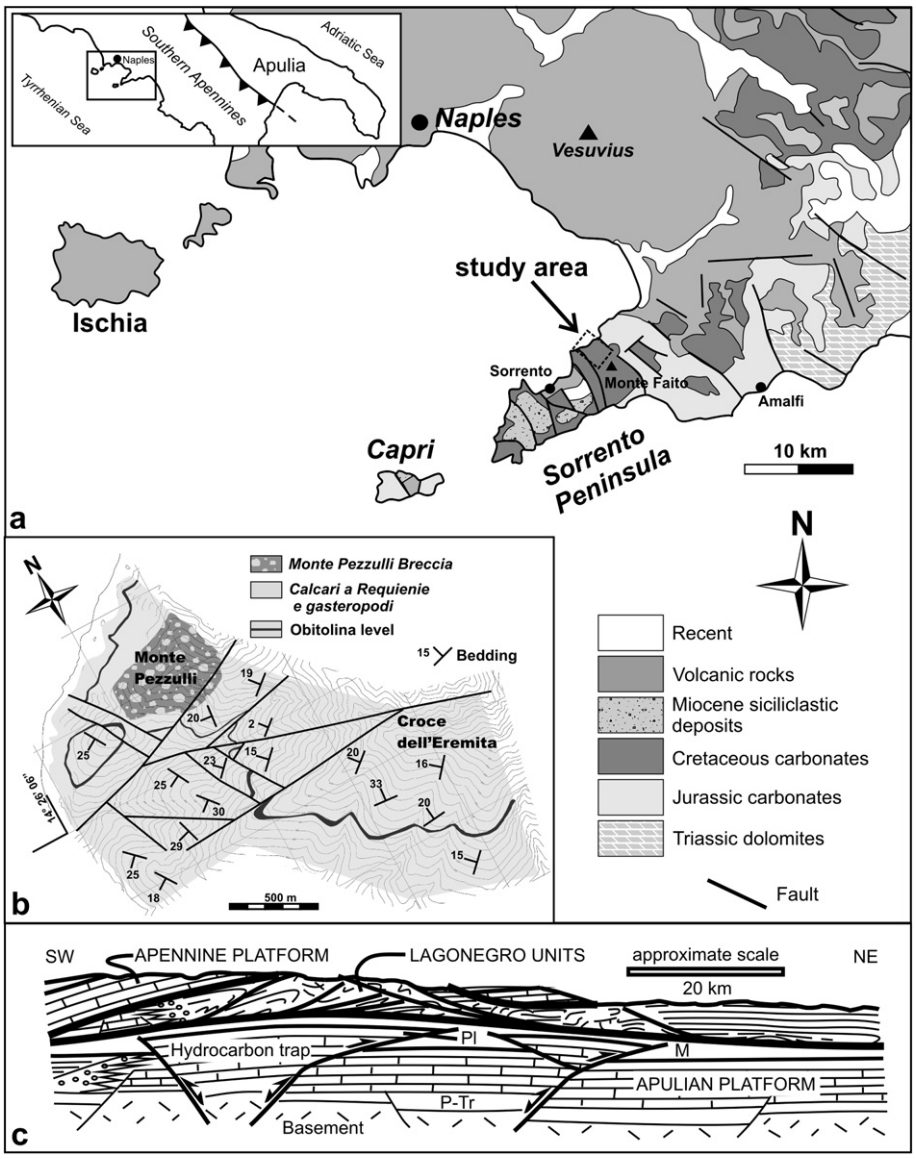

Fig. 1. (a) Geological sketch map of the Naples – Sorrento Peninsula area, showing location of studied fractured carbonates outcrop. (b) Geological sketch map of field study area. (c) Sketch showing depth structure of the southern Apennines (after Mazzoli et al., 2008). Pl: Pliocene siliciclastic beds overlying the Apulian Platform carbonates. M: Melange zone at the base of the allochthon (Mazzoli et al., 2001). P-Tr: Permo-Triassic siliciclastic beds underlying the Apulian Platform carbonates.

et al. (2006). For limestone bed 57, a microscale scan line, about 15 cm long (Fig. 2b), has also been analyzed using a digital microcamera (Proscope). Microscale analysis has been conducted using two magnification levels (50× and 100×). However, good quality images and the data set shown in this paper have been recorded using the lower enlargement (50×).

Table 1
Main parameters of analyzed beds.

Bed no.	Lithology	Mech. layer thickness (cm)	Fracture density apert. ≥0.2 mm (m^{-1})
1	Mudstone	44	14.8
57	Mudstone	45	15.2
66	Fine Dolomite	54	15.4
71	Fine Dolomite	60	12.8
102	Coarse Dolomite	30	17.8
107	Mudstone	55	10.4
118	Coarse Dolomite	50	11.7
120	Coarse Dolomite	50	6.5

3. Analysis of uncertainties

The multi-scale analysis of cumulative data distributions of attributes such as fracture aperture is affected by errors of various nature and origin. A review of the different types of artifacts in fracture analysis has been provided by Ortega et al. (2006), concerning systematic errors occurring at the both extremities of the scale of observation. However, a non-systematic, often more dangerous error is that associated with the uncertainty of the obtained sampling estimates. In order to quantify such an uncertainty, Ortega et al. (2006) suggested using a diagram of fracture density vs. fracture number. A diagram of this type shows how, for increasing fracture number, the mean fracture-density value tends to stabilize and the related 68% confidence interval (which, by definition, is the real segment containing the mean of the whole population with a probability of 68%), obtained from the standard deviation of mean fracture-density values, becomes smaller. The contraction of the confidence interval guarantees a larger reliability of the obtained sampling estimate. An example of such an approach

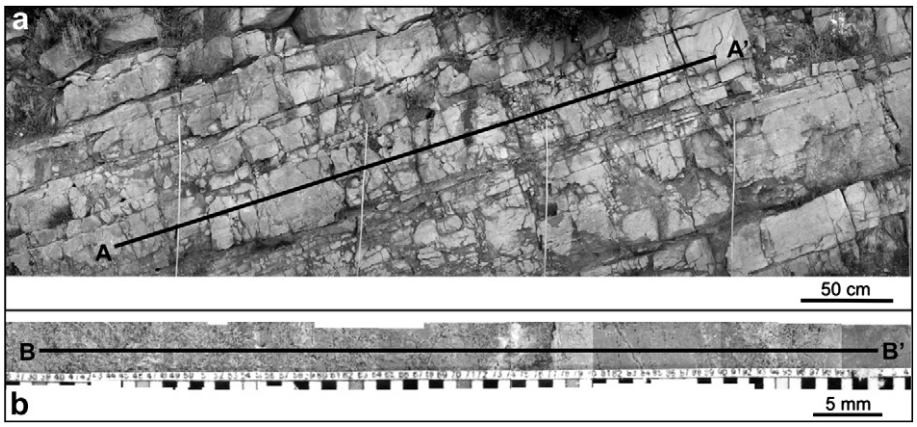

Fig. 2. Examples of analyzed carbonate rocks. (a) Segment of scan line for fracture data collection. (b) Micro-scan line photomosaic from bed 57.

is shown in Fig. 4a where, for an aperture lower threshold of 0.215 mm, the estimated standard deviation is about 10% of the mean value. However, when we consider the uncertainty associated with fracture-density estimates for structures belonging to the same set but with aperture larger or equal to, for example, 2.15 mm, the standard deviation becomes greater than 200% of the mean value (Fig. 4b). In general, cumulative frequency estimates for fractures of larger dimension – and therefore less numerous (data points located toward the right edge in cumulative distribution diagrams) – may be affected by large errors.

Hence the quantification of uncertainties of the cumulative frequency distribution of joint apertures requires the determination of the confidence intervals for fracture density (or, equivalently, mean fracture spacing) for each aperture value.

3.1. Confidence interval determination

The mean confidence interval for cumulative frequency distributions of fracture aperture has been obtained using mean spacing values (S), as this is approximately the inverse of fracture density (F). In fact, considering a scan line of length "L" originating and terminating at two fractures belonging to the analyzed set, the mean spacing is given by: $S = \Sigma_i\, s_i \,/\, (N-1)$. On the other hand, a scan line originating and terminating at random locations would provide a value of mean fracture density of: $F = N/L$. As the number (N) of sampled fractures increases, we obtain: $L \approx \Sigma_i s_i$ and $N \approx N-1$. As the latter two approximations compensate each other, the error becomes negligible already for small N values and therefore we can consider $F \approx 1/S$.

The spacing values show, for all scan lines, a standard deviation stochastically converging toward the mean value as fracture sample size grows. Fig. 5 shows the behaviour of the mean spacing values and related standard deviation as a function of sample size ($n = N-1$) for all fractures detected from the eight scan lines. A ratio of mean value/standard deviation tending to unity is characteristic of fracture sets showing random distribution (Gillespie et al., 1993), i.e. such that the abscissa value for each fracture along the scan line is a uniform aleatoric variable of the [0; L] segment. The associated spacing distribution, based on the probabilistic theory, is described by means of the exponential aleatoric variable, whereas fracture density is a Poisson's aleatoric variable (e.g. Erto, 2004).

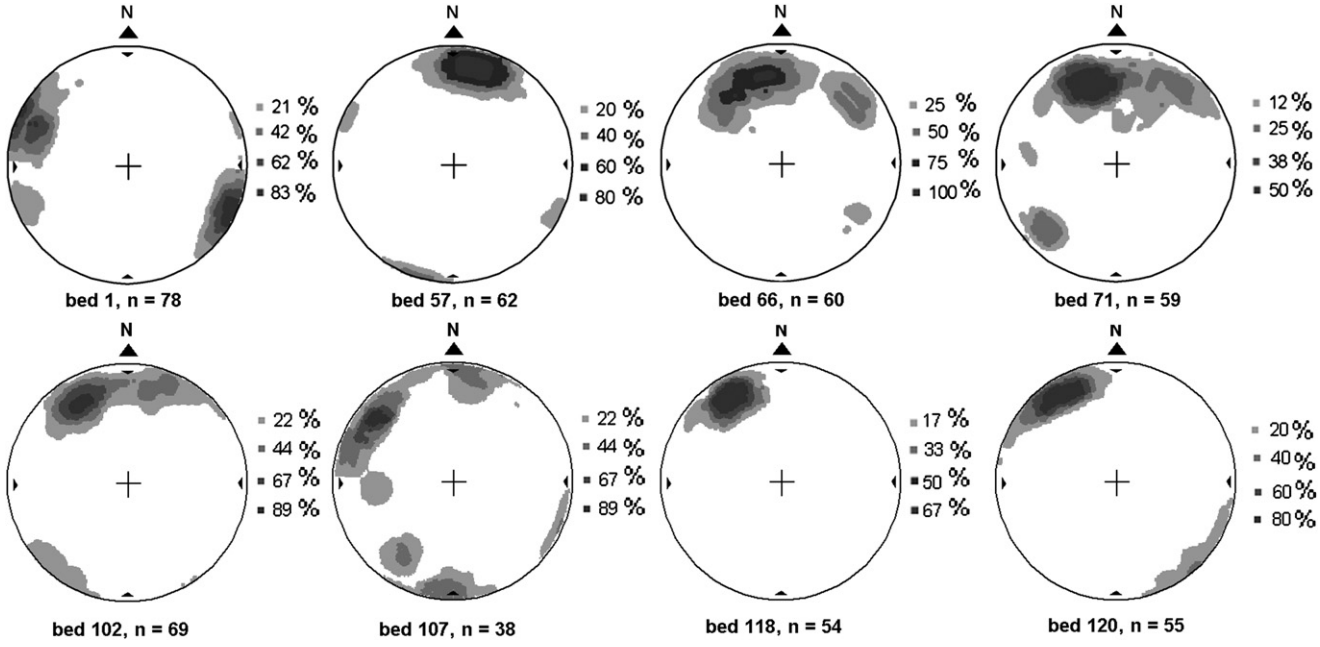

Fig. 3. Orientation data (lower hemisphere, equal area projections of density contour of poles to planes) for measured fractures from all analyzed beds.

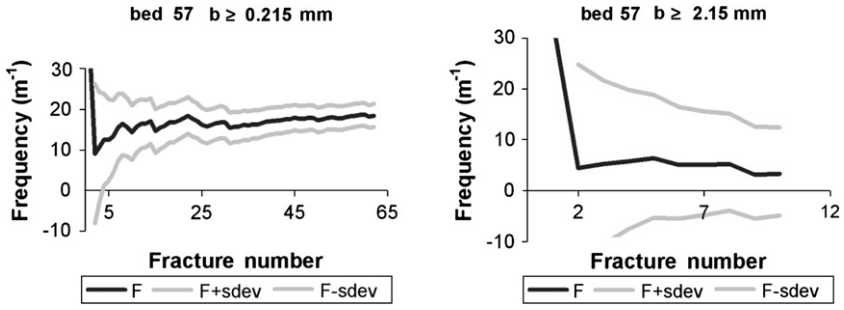

Fig. 4. Uncertainty diagram (68% confidence interval) for fracture-density estimate for the dominant set in bed 57. (a) Aperture > 0.215 mm. (b) Aperture > 2.15 mm.

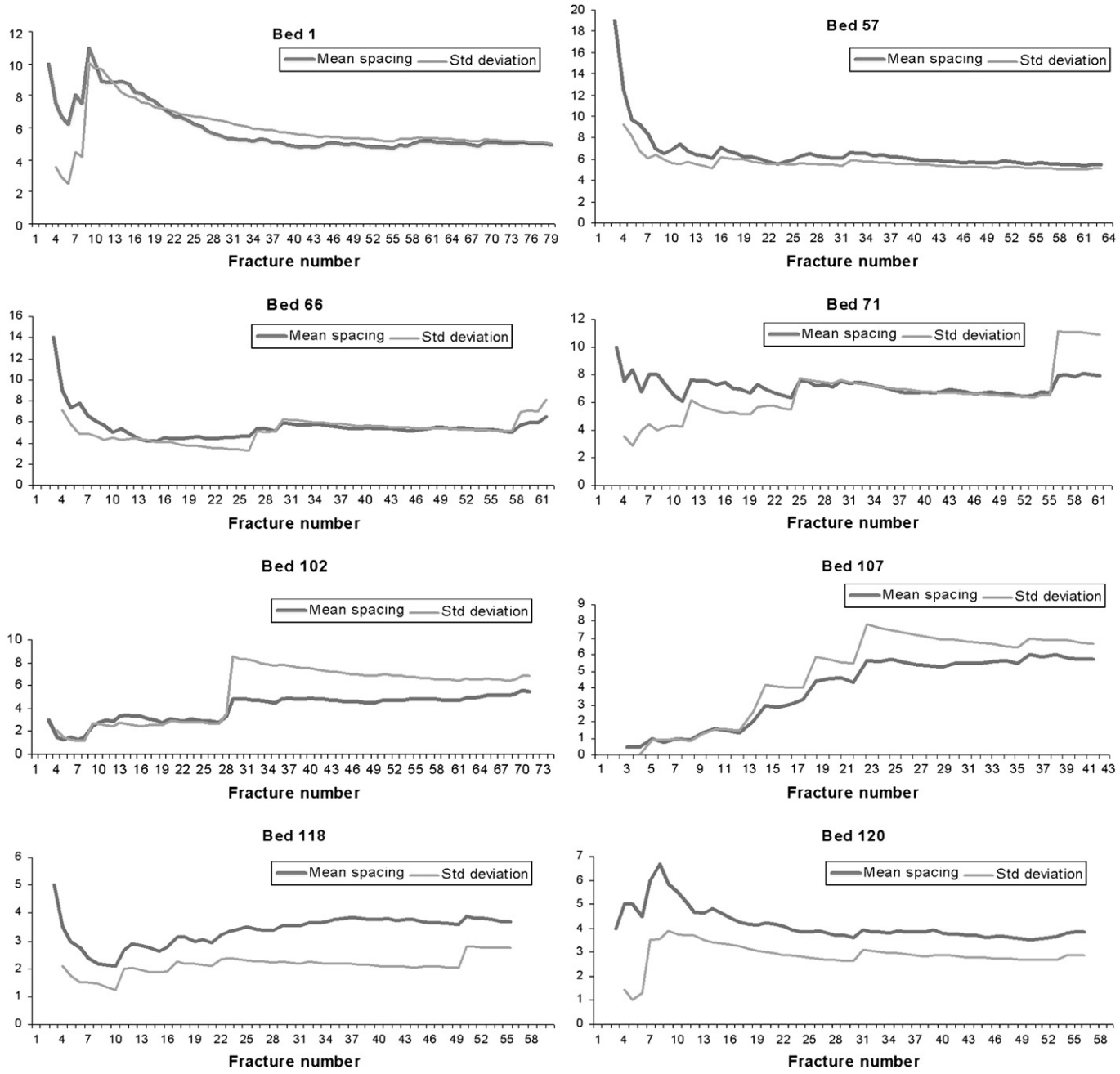

Fig. 5. Mean spacing and standard deviation as a function of fracture number for all beds.

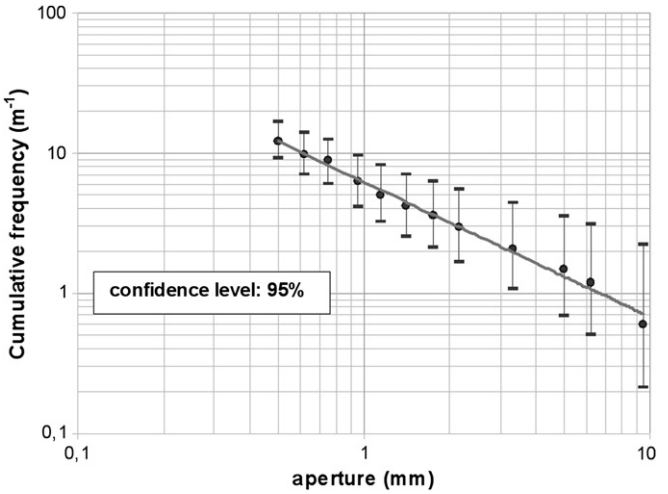

Fig. 6. Log–log diagram of fracture aperture cumulative frequency in bed 57, with 95% confidence intervals obtained using the *exact* method based on Poisson's aleatoric variable. The diagram does not include confidence intervals for aperture values <0.5 mm, as these may be affected by truncation artifacts (whose evaluation is beyond the scope of this paper).

The standard deviation may display local large fluctuations (for spacing values significantly different from the mean value; see bed 102 in Fig. 5); however, it consistently converges toward the mean value. Therefore, it is feasible to use the mean spacing to estimate the standard deviation, as the mean is its most efficient *estimator* (which by definition is that with the least mean square deviation with respect to the real value of the parameter). It should be noted that the criteria used in the diagrams of Fig. 4, involving direct measurement of the standard deviation of the sample means, provide a less efficient *estimator* with respect to that above, because it uses a series of stochastically dependent variables (the mean fracture density obtained for k fractures depends on the mean values obtained for $k-1$, $k-2$ … fractures).

A simple and rapid method to calculate the confidence interval for mean fracture density, for each aperture value, utilizes the determination of the confidence interval of mean spacing. Although we know the probabilistic distribution of the mean fracture density (Poisson's distribution), we suggest an easier way to calculate its confidence interval, based on the application of the *central limit theorem*. This allows us considering the estimated mean spacing as an aleatoric variable with: (i) a normal distribution, (ii) a mean value equal to the mean spacing of the whole population (μ), and (iii) a standard deviation of $\mu/n^{1/2}$. Based on our simulations, a minimum of 20 measurements is sufficient to furnish significant results. Therefore, we impose that the probability – that is the standardized variable $u = (S-\mu)/(\mu/\sqrt{n})$ being comprised within the interval $[-u_{\alpha/2}; u_{\alpha/2}]$ – is equal to the 95%:

$$\Pr\left\{-u_{\alpha/2} < (S-\mu)/(\mu/\sqrt{n}) < u_{\alpha/2}\right\} = 0.95, \tag{3}$$

where: $u_{\alpha/2} = 1.96$ is the value of the normal standard aleatoric variable with probability = 0.025; $S \approx L/N$ is the mean spacing; and $N = n+1$ is the number of fractures detected along the scan line.

The lower limit μ_{low} of the interval is obtained as:

$$u_{\alpha/2} = (S-\mu_{\text{low}})/(\mu_{\text{low}}/\sqrt{n}); \tag{4}$$

therefore:

$$\mu_{\text{low}} = S/(1+u_{\alpha/2}/\sqrt{n}). \tag{5}$$

Similarly, the upper limit μ_{upp} of the interval is obtained as:

$$\mu_{\text{upp}} = S/(1-u_{\alpha/2}/\sqrt{n}). \tag{6}$$

Taking into account that the mean fracture density is given by: $F = N/L \approx 1/S$, and that: $F_{\text{low}} \approx 1/\mu_{\text{upp}}$, $F_{\text{upp}} \approx 1/\mu_{\text{low}}$, and substituting the values in the equations above, we obtain two simple equations for the lower and upper limits of the confidence intervals for mean fracture density, respectively:

$$F_{\text{low}} = \left(1 - 1.96/(N-1)^{1/2}\right)N/L, \tag{7}$$

$$F_{\text{upp}} = \left(1 + 1.96/(N-1)^{1/2}\right)N/L. \tag{8}$$

Equations (7) and (8) permit a rapid calculation of the 95% confidence interval for each value of fracture density in the analysis of cumulative distributions of fracture aperture.

A more precise but less practical method, commonly used in inferential statistics for the determination of the confidence interval of the mean (μ) of the exponential aleatoric variable, consists in the use of the Chi-square aleatoric variable (Erto, 2004). The process is similar to the previous one, with:

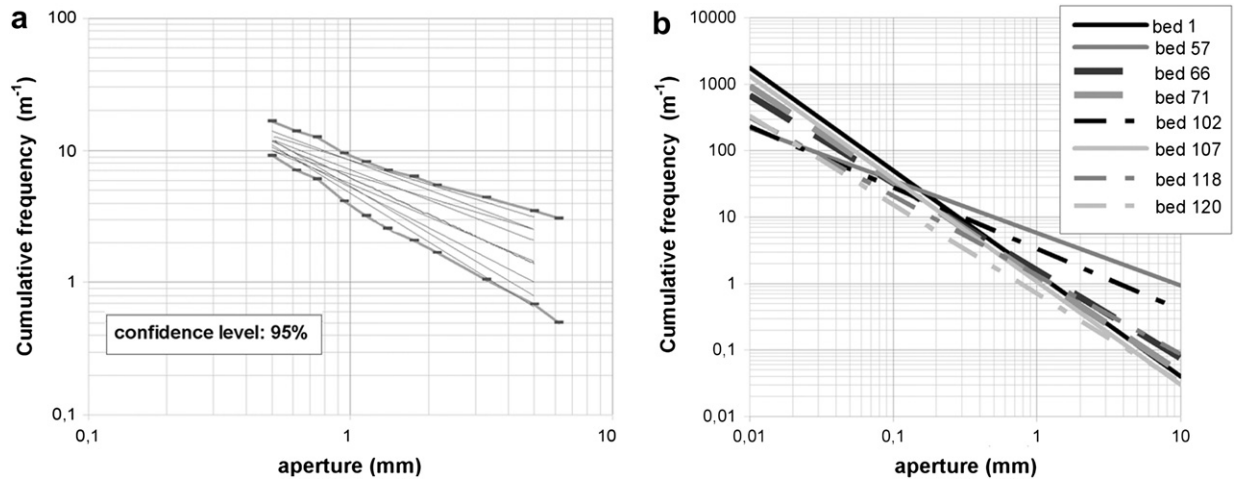

Fig. 7. (a) Simulated power-law curves within 95% confidence intervals for fracture aperture frequency distribution in bed 57. (b) Best-fit power laws for fracture aperture frequency distributions for all (eight) scan lines.

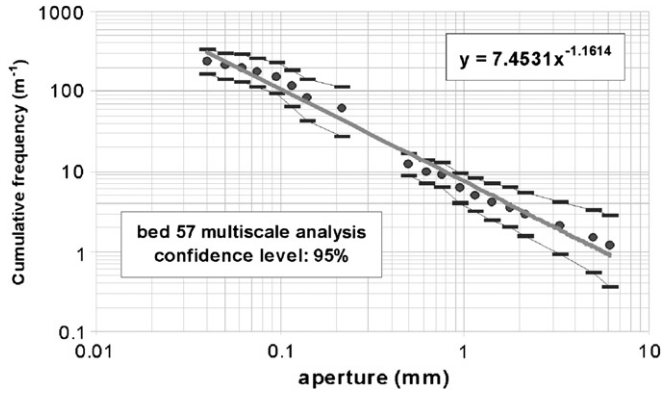

Fig. 8. Log–log diagram of fracture aperture cumulative distribution and 95% confidence intervals obtained by the integration of outcrop and micro-scan line data for bed 57.

$$\Pr\{k1 < 2\,n\,s/\mu < k2\} = 0.95, \tag{9}$$

where $k1$ and $k2$ are the values of the Chi-square aleatoric variable, with a degree of freedom equal to $2n$, to which are associated probabilities 0.025 and 0.975, respectively. We obtain:

$$F_{\text{low}} = k1/2\,n\,S, \tag{10}$$

and

$$F_{\text{upp}} = k2/2\,n\,S. \tag{11}$$

Finally, in case the number of detected fractures is very low (<15–20), it is necessary to use an *exact* method for the evaluation of the confidence interval. To this purpose, we need to take into account that the fracture-density probability distribution, for a fracture set showing a random distribution, is described by Poisson's aleatoric variable (e.g. Erto, 2004). Terming F the estimated mean fracture density and f the fracture density described by Poisson's aleatoric variable (dependent on μ and L), the method consists on imposing $\Pr\{F \le f\} = 0.975$ and solving it numerically in μ, obtaining the lower limit of the confidence interval. Similarly, solving the equation $\Pr\{F \le f\} = 0.025$, the upper limit of the confidence interval is obtained.

Fig. 6 shows the 95% confidence intervals for all values of cumulative frequency associated with the different fracture aperture classes (>0.5 mm), using the *exact* method based on Poisson's aleatoric variable.

4. Implemented scan line fracture analysis

The increasing uncertainty of frequency sampling estimates for progressively larger aperture values may result in significant errors in the estimate of the parameters (exponent and coefficient of the power law) defining the least-squares line in a bi-logarithmic diagram of aperture cumulative frequency vs. aperture values. As an example, Fig. 7a shows a series of possible correlation straight lines, obtained by means of a simulation, for bed 57. Given the confidence intervals associated with this data set, all of the lines could equally be used to approximate the data distribution. For comparison, in Fig. 7b the regression straight lines associated with the cumulative distributions for all eight analyzed carbonate beds are shown. Diagrams (a) and (b) in Fig. 7 point out how the different power laws approximating the data distributions for the different beds could be strongly influenced – or even entirely derive – by the aleatoric error associated with the sampling estimates of aperture cumulative frequencies. In order to avoid such errors, and to reduce the width of the confidence intervals, a much larger amount of data would be needed, therefore requiring very long scan lines encountering several hundreds of fractures. This, besides being extremely time-consuming and anti-economic, would in many instances be inhibited by the lack of suitable outcrop.

A much more efficient method involves carrying out scan line fracture data detection at different scales of observation. Such a multi-scale approach has already been adopted (e.g. Ortega et al., 2006). However, we propose to integrate it with the consideration of the confidence intervals discussed in the previous section. As an example, we include in the analysis the data gathered from a micro-scan line on bed 57, obtained using the microphotocamera (proscope) at a magnification of 50×. The data obtained from the micro-scan line alone constitute a rather small data set. However, when these fracture density data are included in the aperture cumulative frequency diagram, together with the outcrop-derived data, we obtain a significantly reduced uncertainty associated with the parameters (exponent and coefficient) defining the power law (Fig. 8).

5. Concluding remarks

Fracture density at a single location varies as a function of the scale of observation, according to the smallest fracture size included in the analysis. Our analysis points out that the uncertainty in the estimate of the cumulative distribution of fracture aperture data increases for large aperture values. This results in progressively larger confidence intervals for smaller samples – i.e. toward the right in log–log cumulative frequency diagrams, therefore implying a large uncertainty in estimating the slope of the least-squares line (i.e. the coefficient of the power law approximating the data distribution). A significant reduction in the uncertainty is provided by multi-scale analysis and by the integration of micro-scan line data with traditional outcrop-based scan line analysis. A fundamental step in our analysis is represented by the quantification of uncertainties of the cumulative distribution estimates of fracture apertures. This is performed by analyzing in detail the spacing distribution (or, equivalently, fracture-density distribution) features, and by determining the 95% confidence intervals for fracture-density estimates, for each aperture value. Our analysis shows that joints and veins exhibit a random spatial distribution. Consequently, based on probabilistic theory, we can state that fracture density has a Poisson's probability distribution, whereas fracture spacing is characterized by an exponential distribution. A simple and rapid method to calculate the confidence interval for mean spacing (and consequently for fracture density) is based on the application of the *central limit theorem*, considering the estimated mean as an aleatoric variable with normal distribution and mean value equal to the mean spacing of the whole population (μ) and standard deviation of $\mu/n^{1/2}$. Based on our simulations, a minimum of 20 measurements is sufficient to provide significant results. A more precise but less practical method, commonly used in inferential statistics for the determination of the confidence interval of the mean (μ) of the exponential aleatoric variable, consists in the use of the Chi-square aleatoric variable. Finally, in case the number of measured fractures is very low (<15–20), it is necessary to use an *exact* method for the evaluation of the fracture-density confidence interval involving Poisson's probability distribution. Our analysis also points out that, as the standard deviation of fracture spacing stochastically converges toward the mean value, the confidence interval of fracture-density estimates is best obtained by using the mean. The latter is the most efficient *estimator*, i.e. that with the most rapid stochastic convergence toward the standard deviation of fracture spacing. It should be noted that the criteria proposed by Ortega et al. (2006), involving the analysis of the variance of consecutive fracture

frequency estimates, provide a less efficient *estimator* with respect to the mean, because it uses a series of stochastically dependent variables.

Acknowledgements

The paper greatly benefited from thorough and constructive reviews by Luca Micarelli and Aderson Farias do Nascimento. Comments by guest editors Fabrizio Agosta and Emanuele Tondi, and by editor Tom Blenkinsop helped to improve the paper. Financial support by Shell Italia E&P is gratefully acknowledged.

References

Bai, T., Pollard, D.D., 2000. Fracture spacing in layered rocks: a new explanation based on the stress transition. Journal of Structural Geology 22, 43–57.

Barton, C.A., Zoback, M.D., 1992. Self-similar distribution and properties of macroscopic fractures at depth in crystalline rock in the Cajon Pass scientific drill hole. Journal of Geophysical Research 97, 5181–5200.

Barton, C.C., 1995. Fractal analysis of scaling and spatial clustering of fractures. In: Barton, C.C., La Pointe, P.R. (Eds.), Fractals in the Earth Sciences. Plenum Press, pp. 141–178.

Das Gupta, U., 1978. A Study of Fractured Reservoir Rocks, with Special Reference to Mississippian Carbonate Rocks of Southwest Alberta. Ph.D. thesis, University of Toronto.

Erto, P., 2004. Probabilità e statistica per le scienze e l'ingegneria. McGraw-Hill, Milano.

Galluccio, L., Frijia, G., Iannace, A., Mazzoli, S., Parente, M., Vitale, S., Giorgioni, M., D'amore, M., 2008. Diagenesis and petrophysics of dolomite in the "middle" Cretaceous of the Sorrento Peninsula (Southern Apennines). Rendiconti online Società Geologica Italiana 2, 79–84.

Gillespie, P.A., Howard, C.B., Walsh, J.J., Watterson, J., 1993. Measurement and characterization of spatial distributions of fractures. Tectonophysics 226, 113–141.

Gross, M.R., 1993. The origin and spacing of cross joints: examples from the monterrey formation, Santa Barbara coastline, California. Journal of Structural Geology 15, 737–751.

Gross, M.R., Engelder, T., 1995. Strain accommodated by brittle failure in adjacent units of the monterey formation, U.S.A.: scale effects and evidence for uniform displacement boundary conditions. Journal of Structural Geology 17, 1303–1318.

Gudmundsson, A., 1987. Geometry, formation, and development of tectonic fractures on the Reykjanes Peninsula, southwest Iceland. Tectonophysics 139, 295–308.

Heffer, K.J., Bevan, T.G., 1990. Scaling relationships and natural fractures: data, theory and applications. In: Society of Petroleum Engineers, Europec 90, The Hague, October 22–24, SPE Paper 20981, pp. 367–376.

Huang, Q., Angelier, J., 1989. Fracture spacing and its relation to bed thickness. Geological Magazine 126, 355–362.

Johnston, J.D., McCaffrey, K.J.W., 1996. Fractal geometries of vein systems and the variation of scaling relationships with mechanism. Journal of Structural Geology 18, 349–358.

Mandelbrot, B., 1983. The Fractal Geometry of Nature. Freeman and Company, New York.

Mandal, N., Deb, S.K., Khan, D., 1994. Evidence for a nonlinear relationship between fracture spacing and layer thickness. Journal of Structural Geology 16, 1275–1281.

Marrett, R., 1997. Permeability, porosity, and shear-wave anisotropy from scaling of open fracture populations. In: Hoak, T.E., Klawitter, A.L., Blomquist, P.K. (Eds.), Fractured Reservoirs: Characterization and Modeling Guidebook. Rocky Mountain Association of Geologists, pp. 217–226.

Mazzoli, S., Barkham, S., Cello, G., Gambini, R., Mattioni, L., Shiner, P., Tondi, E., 2001. Reconstruction of continental margin architecture deformed by the contraction of the Lagonegro basin, southern Apennines, Italy. Journal of the Geological Society 158, 309–319.

Mazzoli, S., D'Errico, M., Aldega, L., Corrado, S., Invernizzi, C., Shiner, P., Zattin, M., 2008. Tectonic burial and "young" ($<$10 Ma) exhumation in the southern Apennines fold-and-thrust belt (Italy). Geology 36, 243–246. doi:10.1130/G24344A.

Narr, W., 1996. Estimating average fracture spacing in subsurface rock. AAPG Bulletin 80, 1565–1586.

Narr, W., Suppe, J., 1991. Joint spacing in sedimentary rocks. Journal of Structural Geology 13, 1037–1048.

Nelson, R.A., 1985. Geologic Analysis of Naturally Fractured Reservoirs. Gulf Publishing, Houston.

Odling, N.E., Gillespie, P., Bourgine, B., Castaing, C., Chiles, J.P., Christensen, N.P., Fillion, E., Genter, A., Olsen, C., Thrane, L., Trice, R., Aarseth, E., Walsh, J.J., Watterson, J., 1999. Variations in fracture system geometry and their implications for fluid flow in fractured hydrocarbon reservoirs. Petroleum Geoscience 5, 373–384.

Ortega, O., Marrett, R., Hamlin, S., Clift, S., Reed, R., 1998. Quantitative macrofracture prediction using microfracture observations: a successful case study in the Ozona Sandstone, west Texas (abstract). In: AAPG Annual Meeting Program, vol. 7, A503.

Ortega, O., Marrett, R., 2000. Prediction of macrofracture properties using microfracture information, Mesaverde Group sandstones, San Juan basin, New Mexico. Journal of Structural Geology 22, 571–588.

Ortega, O., Marrett, R., Laubach, E., 2006. Scale-independent approach to fracture intensity and average spacing measurement. AAPG Bulletin 90, 193–208.

Pascal, C., Angelier, J., Cacas, M.-C., Hancock, P.L., 1997. Distribution of joints: probabilistic modeling and case study near Cardiff (Wales, U.K.). Journal of Structural Geology 19, 1273–1284.

Price, N.J., 1966. Fault and Joint Development in Brittle and Semibrittle Rocks. Pergamon Press, Oxford.

Sanderson, D.J., Roberts, S., Gumiel, P., 1994. A fractal relationship between vein thickness and gold grade in drill core from La Codosera, Spain. Economic Geology 89, 168–173.

Sinclair, S.W., 1980. Analysis of Macroscopic Fractures on Teton Anticline, Northwestern Montana. M.S. thesis, Texas A&M University.

Shiner, P., Beccacini, A., Mazzoli, S., 2004. Thin-skinned versus thick-skinned structural models for Apulian carbonate reservoirs: constraints from the Val D'Agri fields. Marine and Petroleum Geology 21, 805–827.

Wu, H., Pollard, D.D., 1995. An experimental study of the relationship between joint spacing and layer thickness. Journal of Structural Geology 17, 887–905.